Check for updates

Water Science & Technology

IWA PUBLISHING

© 2022 The Authors

Water Science & Technology Vol 86 No 11, 2777 doi: 10.2166/wst.2022.381

Green infrastructure drainage of a commercial plaza without directly connected impervious areas: a case study

Hendrik Rujner*, Günther Leonhardt, Kelsey Flanagan, Jiri Marsalek and Maria Viklander

Department of Civil, Environmental and Natural Resources Engineering, Urban Water Engineering, Luleå University of Technology, Luleå 971 87, Sweden
*Corresponding author. E-mail: hendrik.rujner@ltu.se

HR, 0000-0002-2321-164X; GL, 0000-0003-0367-3449; KF, 0000-0003-4327-5613; JM, 0000-0001-9938-8217; MV, 0000-0003-1725-6478

ABSTRACT

A paired-catchment study of two adjacent commercial areas in northern Sweden, one with Green Infrastructure (GI) storm drainage and the other with a conventional storm sewer system, served to evaluate the hydrological performance of both drainage systems and demonstrate advantages of GI. The GI catchment avoided directly connected impervious areas by diverting runoff from a parking lot to a cascade of three infiltration features, a fractured rock strip draining onto a sloping infiltration area, followed by a collector swale. Both catchments were monitored over 4 years by measuring rainfall, runoff and, in the vicinity of the swale, soil water content and groundwater levels. For frequent storms, the median GI efficiencies in reducing runoff volumes and peak flows, and extending peak flow lags, were 96, 99 and 60%, respectively, compared to conventional drainage. The storm rainfall depth, initial soil water content, increases in intra-event soil water storage and groundwater levels had statistically significant effects on either runoff volume or peak flow reductions. No effects were found for storm rainfall intensity and duration, antecedent dry days, and initial groundwater levels. The study demonstrated that GI drainage can be successfully applied even in the challenging environment of a subarctic climate.

Key words: commercial runoff, directly connected impervious area (DCIA), green infrastructure (GI), low impact development (LID) monitoring, semi-natural stormwater control

HIGHLIGHTS

- The hydrology of Green Infrastructure and conventional DCIA drainage was monitored over 5 years.
- The GI significantly reduced runoff volumes, peak flows and increased lag times compared to conventional drainage.
- Initial soil water content, increases in intra-event soil water storage, and groundwater levels near the swale affected runoff reductions.

INTRODUCTION

One of many challenging tasks in urban land development is the design of drainage of suburban shopping plazas with large roof and parking lot surfaces with more sustainable and resilient solutions. Their drainage was directly connected to storm sewers even in recent practice. Such surfaces are called 'directly connected impervious areas' (DCIAs), convert almost all rainfall into runoff, and contribute to the deterioration of the natural environment in the receiving waters through the 'urban stream syndrome' (Walsh *et al.* 2005; Schueler *et al.* 2009; Obropta & Del Monaco 2018). With respect to the catchment hydrology, the total catchment imperviousness (TCI) was identified as an indicator of urbanization impacts on catchment hydrology (Roy & Shuster 2008; Jacobson 2011), or an approximate indicator of the receiving stream quality (Schueler *et al.* 2009). These impacts can be mitigated by Green Infrastructure (GI), which was broadly defined in the US Clean Water Act as the range of measures, both natural and man-made, mimicking natural processes that store, reuse, infiltrate, or evapotranspirate stormwater and thereby reduce flows to sewer systems, or receiving surface waters (USEPA 2020). During the last two decades, numerous studies of GI performance were reported, as documented e.g. in Ying *et al.*'s review (2021) referring to almost 2,200 studies, with the highest number of studies focusing on stormwater management employing mostly natural solutions in urban settings and temperate or subtropical climates. Furthermore, as noted by Taguchi *et al.*

This is an Open Access article distributed under the terms of the Creative Commons Attribution Licence (CC BY 4.0), which permits copying, adaptation and redistribution, provided the original work is properly cited (http://creativecommons.org/licenses/by/4.0/).

Downloaded from http://iwaponline.com/wst/article-pdf/86/11/2777/1149397/wst086112777.pdf
by LULEA TEKNISKA UNIVERSITET user

(2020), GI drainage is designed for specific performance and may cause 'unintended' issues such as groundwater contamination by deployment without full knowledge of operational or environmental consequences.

To expand the knowledge base of GI options in, and experience with, a cool temperate climate and in the environs of urban areas, the authors partnered with a municipality in Northern Sweden to examine the hydrological performance of a 0.75 ha extension of an existing suburban commercial plaza (built in the early 2010s) having drainage designed according to GI principles. This was achieved by reducing the DCIA of the plaza extension catchment to zero, by diverting runoff from the asphalt parking lot onto a pervious strip (mostly gravel and crushed rock) followed by a sloping infiltration area, and collecting residual runoff in a swale, which eventually drains into a local storm sewer system.

Benefits of reducing DCIA of urban catchments were studied by Obropta & Del Monaco (2018), who concluded that stormwater controls should focus on DCIAs, rather than the total catchment imperviousness (TCI), because it is the DCIA, typically responsible for high surface runoff and pollutant discharges, that harms the local receiving waters. Hydrological consequences of diverting runoff from impervious surfaces, or replacing them with pervious ones, were addressed in a number of studies, based on hydrological modelling with uncalibrated models, which introduces uncertainties into the results produced (e.g., Alley & Veenhuis 1983; Roy & Shuster 2008; Jacobson 2011; Silva & Silva 2020). In our study, there was a unique opportunity to compare the hydrological performance of the GI drainage facility against that of the older plaza section with conventional drainage and directly connected impervious areas. The objectives of our study can be summarized as follows: (i) Using a paired-catchments experimental design and field measurements of rainfall and runoff, compare the hydrological performance of GI drainage, with disconnected impervious areas, against that of adjacent conventional drainage with high DCIA, and (ii) elucidate the formation of runoff in GI drainage by interpreting adjunct data from the GI site on groundwater levels and soil water content.

METHODOLOGY

Location and climate of the study sites

The conventional drainage system (CD) and the GI drainage sites were located in a suburban commercial plaza near the City of Skellefteå, Northern Sweden (64° 46′ 5.36″N, 21° 1′ 6.43″E) (Figure 1). According to the Köppen-Geiger classification, the local climate was characterized as subarctic (code: Dfb; Beck *et al.* 2018), with a long-term annual average precipitation of 648 mm, of which a considerable amount is snow during the winter months (35–40% snow water equivalent (SMHI 2019)) and the annual average temperature is 2.2 °C, with annual mean minima of −29.6 °C in winter and annual mean maxima of 27.8 °C in summer. The local soils and geology can be described as postglacial sand and till. The hydraulic conductivity of unsorted glacial sediments in this region was estimated as 1×10^{-6} to 1×10^{-8} m/s (0.36–0.0036 cm/h) (SGU 2018), but may not reflect fully the actual infiltration rates at the study site with soil conditions altered by construction.

Study catchments' characteristics

The assessment of GI drainage was carried out by a paired-catchment comparison, in which the GI drainage site was compared to a nearby catchment served by the conventional storm sewer system. Both catchment boundaries were delineated using a detailed elevation model combining two levels of elevation data: National airborne laser scanning data (resolution 0.5×0.5 m) and individual GPS-based survey data (± 0.02 m). Where needed, corrections were made based on visual field inspections of structures that may affect flow trajectories on the scale studied, such as humps, curbs and pavement irregularities. Both catchments are described below.

Green infrastructure drainage catchment

The GI study catchment has an irregular shape and slopes from the southern boundary, formed by a building wall and a low asphalt hump, in the northerly direction (Figure 2). The upper-most part of the catchment is formed by an asphalt parking lot, which was built on a levelled rock outcrop. The runoff contributing part of the parking lot is about 0.48 ha and was delineated by asphalt humps. At the downstream end of the parking lot is a strip of gravel, about 7 m wide. Further north, the catchment continues by a northerly sloping area with a surface cover formed by patches of mixed debris (gravel and rocks) and native soils with sparse vegetation, connected along the bottom to a 70 m long roadside drainage swale (see Figures 1 and 2). The municipal planners intended to preserve the gravel strip, sloping area and the swale, without any landscaping modifications, for natural infiltration of runoff, before it enters the downstream storm sewer system draining the older part of the plaza. The surface cover of the runoff contributing area is summarized in Table 1.

Downloaded from http://iwaponline.com/wst/article-pdf/86/11/2777/1149397/wst086112777.pdf
by LULEA TEKNISKA UNIVERSITET user

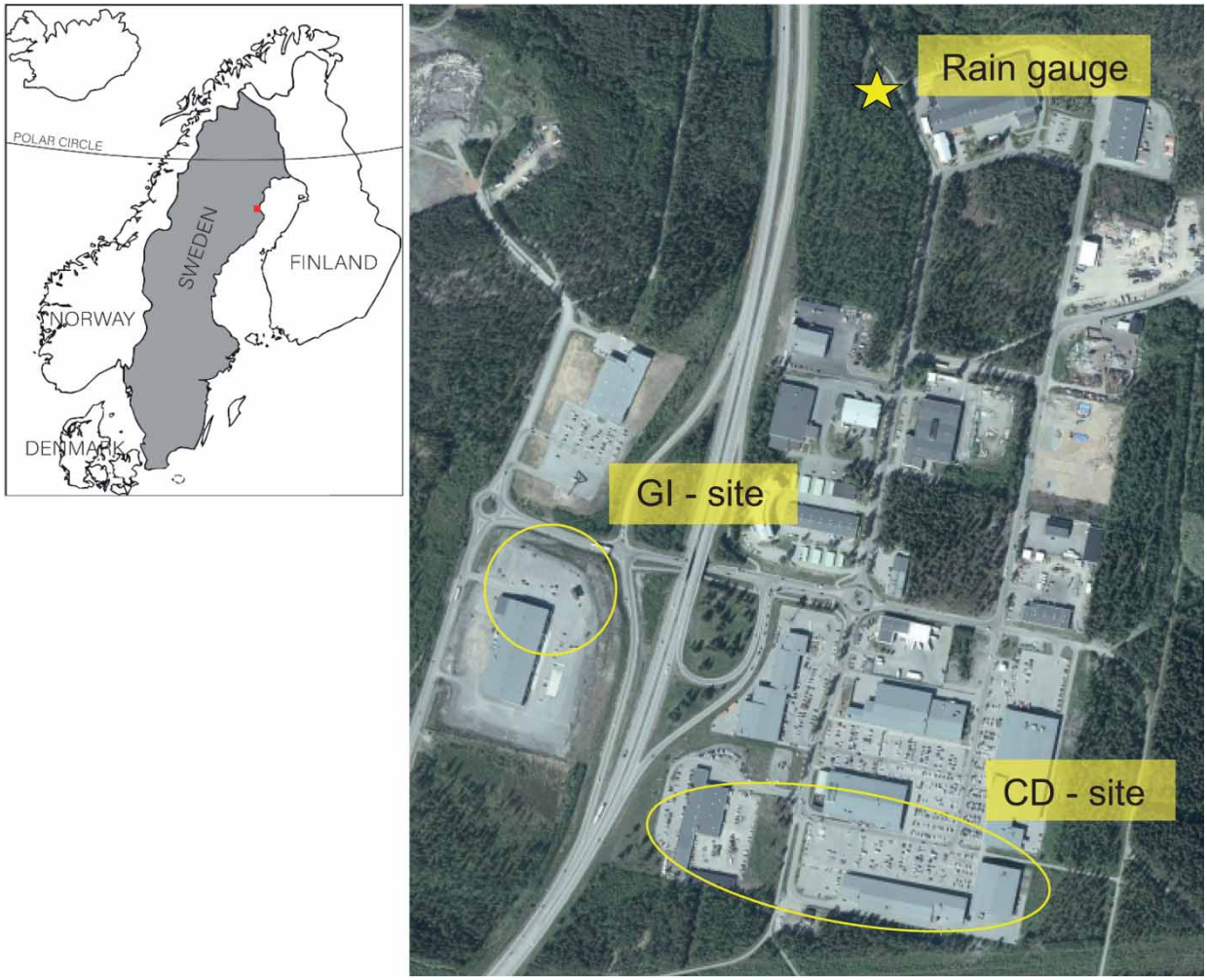

Figure 1 | Map showing locations of the two study sites, GI and CD, and the rain gauge.

Surface runoff leaving the pavement is largely absorbed by the gravel strip and converted into a preferential flow that would either infiltrate into the soil underneath, or continue down the slope as an interflow. At the bottom of the slope is a runoff collecting swale, with channel composed of a mixture of till, soil and gravel. As reported by the Swedish Geological Survey (SGU), the bedrock can be found in this region at depths of 2–4.5 m and acts as a confining layer for shallow groundwater. The ruderal vegetation, which colonized the site after construction, further developed during the monitoring period.

Immediately downstream of the study catchment boundary, the drainage swale discharges via a drop manhole into the existing storm sewer system, preventing water ponding.

Conventional drainage catchment

The second studied catchment, with a runoff contributing area of 2.54 ha, is located in the proximity (300 m) of the GI site. The CD site is 96% impervious (all DCIAs) and comprised two asphalt parking lots and roofs of several large commercial buildings, with the remaining 4% classified as pervious areas. The catchment is drained by conventional curb and gutter drainage discharging into a storm sewer system. The main storm sewer draining the CD site is a 400 mm concrete pipe with an average slope of 2% and the full-bore flow capacity of 0.3 m^3/s. The same storm sewer collects drainage from building foundation drains and, consequently, carries baseflow. Figure 1 provides layouts of both catchments studied and depicts land covers in the study area.

Downloaded from http://iwaponline.com/wst/article-pdf/86/11/2777/1149397/wst086112777.pdf
by LULEA TEKNISKA UNIVERSITET user

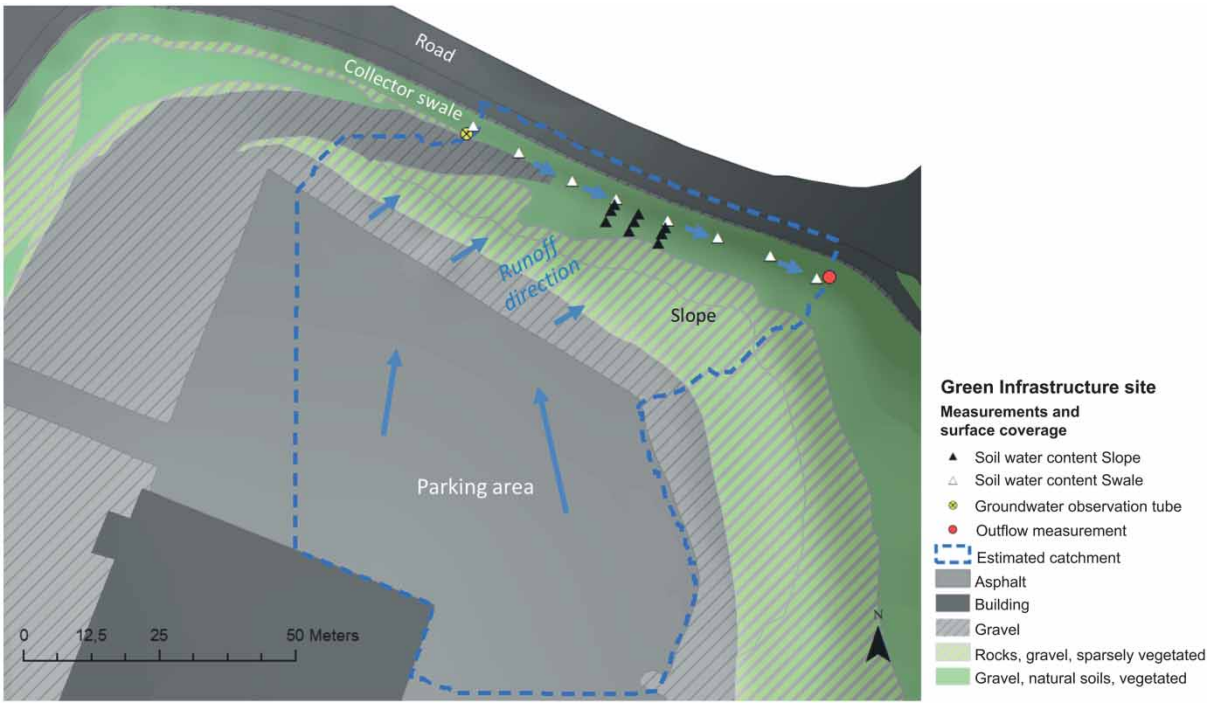

Figure 2 | Detailed overview of the GI site with locations of measurement sensors for groundwater, soil water content and runoff outflow.

Table 1 | GI and CD catchments' characteristics

			Catchment surface cover (%)			
			Impervious			
Study catchment	Total catchment area (ha)	Average slope (%)	Roofs	Pave-ment	DCIA (Directly connected impervious areas)	Pervious (Green)
Green infrastructure drainage (GI)	0.75	8.2	0	64[a]	**0**	36
Conventional stormwater drainage (CD)	2.54	2.3	35	61	**96**	4

[a]Paved subareas discharge onto pervious subareas, hence they are not directly connected to the monitored catchment.

Monitoring equipment and methods

Hydrometeorological data was collected during 2015–2019. Rainfall, runoff flow rate, soil water content, groundwater level, relative humidity and air temperature were monitored as specified in Table 2. Rainfall was measured by a weighing bucket rain gauge located about 800 m north of both study sites (see Figure 1), and runoff discharge from the CD catchment was measured by an area-velocity flow meter installed in a downstream sewer line. At the GI site, outflow from the swale was measured by a long-throated flume, with a known stage-discharge rating curve. Flow depths were measured by a pressure transducer and converted to flow rates by means of the rating curve. For operational reasons, swale flow measurements were conducted only during the snow-free seasons, without freezing temperatures, usually from May to November.

Soil water content was measured with 22 30-cm long water content reflectometers placed along the swale bottom and on side slopes at various depths. Simultaneously, the atmospheric relative humidity and temperature were also recorded. The water table depth was monitored in a groundwater observation riser pipe, installed at the upstream end of the swale, and equipped with a pressure transducer data logger. The locations of measuring devices are shown in Figure 2.

Downloaded from http://iwaponline.com/wst/article-pdf/86/11/2777/1149397/wst086112777.pdf
by LULEA TEKNISKA UNIVERSITET user

Table 2 | Summary of hydrological factors and response variables studied

Factor/response variable	Abbreviation	Units	Comments
Hydrological factors			
Rainfall depth	*P*	mm	Events with rainfall depth > 0.9 mm and duration ≥ 1 hour
Rainfall duration	*Dur*	Hours	Duration of the event defined by the absence of any rainfall 6 hours before and after the event
Rainfall intensity	*i-5*	mm/h	Maximum rainfall intensity during a 5-minute interval
Average rainfall intensity	*i-avg*	mm/h	Average rainfall intensity of event
Antecedent dry days	*ADD*	Days	Cumulative time with no rain prior to the event
Initial groundwater level	*IGL*	cm below the ground	Groundwater level at the GI site in the last time interval just prior to the event; calculated as the depth below the ground surface
Intra-event maximum groundwater level	*MGL*	cm below the ground	Maximum groundwater level
Initial soil water content	SWC_i	Vol.-%	
Intra-event relative change of soil water content	*ΔSWC*	[-]	
Temperature	*T*	degC	
Relative humidity	*RH*	[-]	
Hydrologic response variable			
Normalized runoff depth	*V*	mm	Cumulative runoff outflow measured at the drainage outlet was divided by the respective catchment area of 25,400 m^2 or 7,500 m^2, to yield the normalized runoff depth *V*
Normalized peak flow	q_{max}	L/s/ha	Event peak discharge, *q*, per unit area (ha), i.e., *q* was divided by the catchment areas of 2.54 and 0.75 ha, respectively
Peak lag	t_{lag}	hours	Lag between the rainfall peak and the corresponding flow peak, if identifiable. Otherwise the second or third peak was used, if there was continuing flow
Volumetric runoff coefficient	C_v	–	Event (runoff volume)/(rainfall volume)

Data processing and quality control

The rainfall time series was discretized into individual storm events based on the following criteria: (i) A minimum inter-event dry period of 6 hours, (ii) rainfall depths ≥0.9 mm, and (iii) durations ≥ 1 hour to select distinct events and eliminate minor events producing obscure runoff hydrographs.

Using the measured flow rates and rainfall intensities, the event hydrographs and hyetographs were plotted, visually examined for potential errors and then used to calculate rainfall and runoff characteristics needed in further analysis. The storm sewer monitored at the CD site conveyed a variable baseflow, and consequently, a hydrograph separation procedure, based on the constant slope method (Dingman 2002), was applied to individual events. Such adjustments were not needed at the GI site.

Rainfall parameters needed in further analysis included the total depth and duration, and average and maximum rainfall intensities. The corresponding average return periods of 5-min durations were calculated from the statistical relationships published in the Swedish national guide on rain intensity–duration–frequency curves (Dahlström 2010). Hydrograph parameters of interest included the total runoff depth, peak flow rate, and the peak-to-peak lag time between the rainfall hyetograph and runoff hydrograph, and were determined following the procedures in Hood *et al.* (2007). In cases of multiple corresponding rainfall and runoff peaks, only the highest corresponding peaks were chosen.

Data on event antecedent conditions, such as the initial groundwater level (IGW) and the initial soil water content (SWC_i), were extracted directly from data records according to the time stamps at the beginning of the rainfall event. For SWC_i values, spatial averages were calculated to reduce uncertainties caused by spatial variability of moisture in the underlying soil.

Downloaded from http://iwaponline.com/wst/article-pdf/86/11/2777/1149397/wst086112777.pdf
by LULEA TEKNISKA UNIVERSITET user

To elucidate the role of soil saturation in runoff formation, the change of soil water content during an event, in relation to the sites with a complete SWC spectrum, was calculated as a relative change of saturation:

$$\Delta SWC = \frac{SWC_{max} - SWC_i}{SWC_{avg,\,max} - SWC_{avg,min}} \tag{1}$$

where SWC_i is the initial soil water content, SWC_{max} is the event maximum soil water content, $SWC_{avg,\,min}$ is the site's minimum soil water content, averaged for sensors measuring in depth range 0–30 cm (4.8 Vol.-%), and $SWC_{avg\,max}$ is the site's maximum soil water content, averaged for sensors 0–30 cm (41.1 Vol.-%), during the measurement period. A list of all parameter variables is shown in Table 2.

In hydrometric measurements, uncertainties and errors are typically associated with the functioning and maintenance of measuring devices, and the subsequent data processing (Muste *et al.* 2012). In our study, the effects of occurrences of sensor drift, movement during severe runoff events, or clogging/blinding on flow sensors were minimized by frequent inspections, sensor cleaning and placement corrections, and instrument calibrations. Special attention was paid to the data validation, and when inconsistencies in sensor readings, affecting rainfall/runoff event data, were identified and could not be reconciled, the corresponding data was excluded from further analysis.

Statistical analysis of hydrological performance

Basic statistical analysis was applied to analyse the hydrological parameters and compare the hydrological performance of the GI catchment to the 'reference' CD catchment. Toward this end, four drainage performance indicators were chosen and computed as summarized below:

Event volumetric runoff coefficient: $C_v = \frac{V}{P}$ [dimensionless] (2)

Event runoff volume reduction: $e_V = 1 - \frac{V_{GI}}{V_{CD}}$ [dimensionless] (3)

where V is the normalized event runoff depth in mm, and P is the normalized rainfall depth in mm. In the hydrological conditions studied, the measured swale outflow volume may exceed the inflow volume calculated from the runoff contributing area and the event rainfall, thus producing $C_v > 1$. These seemingly physically anomalous results are explored in the discussion. Finally, e_V is the indicator variable of volume reduction [-], and V_{GI} and V_{CD} are the normalized runoff volumes from the GI and CD sites, respectively.

Event peak flow reduction: $e_q = 1 - \frac{q_{max,\,GI}}{q_{max,\,CD}}$ [dimensionless] (4)

where e_q is the indicator variable of runoff peak flow reduction [dimensionless], and $q_{max,\,GI}$ and $q_{max,\,CD}$ are the normalized runoff peaks in L/s/ha from the GI and CD sites, respectively.

The event peak lag time was defined here as the time difference between the event peak rainfall intensity and the event runoff peak discharge:

Event peak lag time: $t_{lag} = \frac{t_{q_{max}} - t_{p_{max}}}{60}$ (5)

where t_{lag} is the event peak lag time [hours], $t_{p_{max}}$ is the time of the rainfall intensity peak [min], $t_{q_{max}}$ is the time of the corresponding flow peak [min], and 60 is a conversion factor.

Event peak lag reduction: $e_{lag} = 1 - \frac{t_{lag\,GI}}{t_{lag\,CD}}$ (6)

where e_{lag} is the indicator variable of peak lag reduction [dimensionless], $t_{lag\,GI}$ is the peak lag at the GI site, and $t_{lag\,CD}$ is the peak lag at the CD site.

Downloaded from http://iwaponline.com/wst/article-pdf/86/11/2777/1149397/wst086112777.pdf
by LULEA TEKNISKA UNIVERSITET user

The significance of differences in the normalized runoff depths (V), specific peak flows (q_{max}) and event lag times was determined by a paired comparison applying the non-parametric Wilcoxon sign-rank test (Minitab 18 2010). Non-exceedance probability plots were also produced to elucidate the differences in catchment response for the volumetric runoff coefficient, the event peak specific discharge (i.e., the discharge per catchment unit area), and the peak lag time using the Minitab 18 software.

Hydrological performance of the GI site: analysis of influential factors

To consider the interdependence of hydrological factors controlling the runoff response at the GI site, correlations between parameters were tested using the Spearman rho test with a significance threshold of $p \leq 0.05$. The relationships between the hydrologic performance indicators and likely influential factors at the GI site were also explored using scatter plots of each hydrological factor versus the performance indicators.

RESULTS

Sampled storm events

Rainfall characteristics

In total, 60 recorded rainfall events, including 56 with complete data for both study sites, passed the selection criteria and were used in the study. An overview of rainfall characteristics, arranged according to the total rainfall into six classes, is shown in Table 3 and summarized below. Rainfall depths varied from 0.9 to 46 mm (median 5.7 mm, median absolute deviation = 3.6 mm). Maximum 5-min rainfall intensities ranged from 1.4 to 85.0 mm/h (median 8.0 mm/h), while storm durations ranged from 1 to 40 hours. The majority of the events had short return periods ($p < 1$ month), but two events exceeded the return period of 1 year: 20 August 2017 ($p = 2.8$ years) and 14 August 2019 ($p = 4.5$ years). Antecedent dry periods ranged from 0.3 to 11.4 days.

Initial temperatures and relative humidity, at the storm event onset, varied between 1.1 and 25.7 °C and between 43 and 100%, respectively.

Runoff hydrographs

CD runoff

All 60 rainfall events produced discharge from the drainage outlet of the CD site, with hydrographs consistently mimicking the shape of hyetographs, and only minor variations in runoff attenuation or lag time (see Figure 3(a)–3(d)). The event example 7/9/15 shows consistently higher flow rates at the GI site, with the exception of the main hydrograph peak, and continually elevated flows over the recession limb. Event 9/9/17 shows a significant peak flow mitigation and flow attenuation, which was less pronounced towards the end of the event. Event 9/18/17 represents a low-intensity, long-lasting rain event, during which the GI runoff was consistently below the CD runoff. Example event 8/14/19 represents a high-intensity storm, during which the first hyetograph peak was completely retained by the GI site and the second (main) peak was still three times reduced in comparison to the CD peak flow.

The calculated event volume-based runoff coefficients ranged from 0.38 to 1.65 (see Table 5), with a median of 0.87, which is within the range of typical published average values for commercial urban sites (0.70–0.95; City of Saskatoon 2012). Both findings demonstrate the expected hydrologic response for such a small, impermeable catchment. Four event volumetric

Table 3 | Summary of characteristics of the rainfall events used in the study

Number of storms	Rainfall depth, *P* (mm)	Average event rainfall intensity, *i-avg* (mm/h)	5-min peak rainfall intensity, *i-5* (mm/h)	Median duration, *Dur* (h)
25	> 0.9–5	0.6	6.9	7.7
17	> 5–10	0.7	13.4	11.4
9	> 10–20	1.8	17.9	16.4
4	> 20–30	1.5	11.2	27.0
2	> 30–40	1.4	20.5	28.1
3	> 40	1.6	17.6	33.3

Downloaded from http://iwaponline.com/wst/article-pdf/86/11/2777/1149397/wst086112777.pdf
by LULEA TEKNISKA UNIVERSITET user

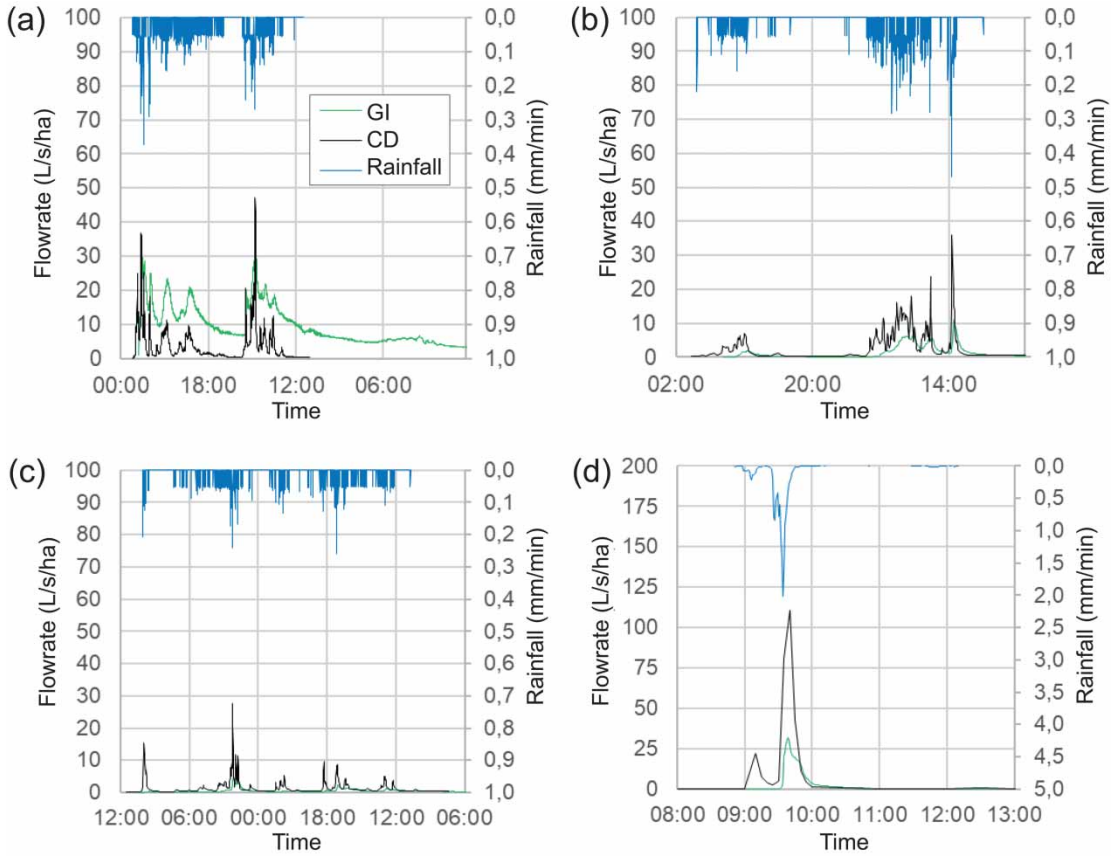

Figure 3 | Examples of rainfall-runoff hydrographs: (a) Event 7/9/15 ($P = 45.3$ mm, $Dur = 33.3$ h); (b) Event 9/9/17 ($P = 33.8$ mm, $Dur = 36.8$ h); (c) Event 9/18/17 ($P = 27.9$ mm, $Dur = 69.9$ h); and, (d) Event 8/14/19 ($P = 15.4$ mm, $Dur = 18.5$ h). Note the different scale (compared to panels a–c).

runoff coefficients exceeded the value of 1; these were statistical outliers associated with anomalous conditions characterized by flow contributions of foundation drains and subsurface inflows from outside the catchment boundaries, as discussed in 'Statistical analysis of hydrological performance' section. The stormwater pipe capacity near the monitoring point was exceeded during two events: 08/19/17 (Figure 3(c)) and 08/14/19 (Figure 3(d)), which affected the instrument readings of the flow rate (set for open channel flow, rather than surcharged pressurized flow) and thereby created statistical outliers. While the latter event represented a high-intensity storm, the former event was just an average storm. Runoff characteristics for the CD and GI sites are summarized in Table 4.

Table 4 | Descriptive statistics of hydrologic variables for the CD and GI sites

Hydrologic Variable	Median	Minimum	Q1[a]	Q3[b]	Maximum
ADD (days)	1.55	0.3	0.73	2.30	11.4
IGL (cm b.g.)	132	18	101.75	201.5	301
MGL (cm b.g.)	94.5	0	15.3	176.8	300
SWC_i (Vol.-%)	24.7	16.5	22.7	27.8	30.8
ΔSWC (Vol.-%)	2.2	0	0.5	4.7	11.2
T (degC)	11.7	1.1	8.9	15.4	25.7
RH	88	43	70	98	100

[a]Q1 is the median of the lower half of the data set.
[b]Q3 is the median of the upper half of the data set.

Downloaded from http://iwaponline.com/wst/article-pdf/86/11/2777/1149397/wst086112777.pdf
by LULEA TEKNISKA UNIVERSITET user

GI runoff

At the GI site, 37% of the 60 sampled events generated no runoff, which is in agreement with earlier references (e.g. Davis *et al.* 2012). This was usually the case for minor or intermediate storms (0.9–18.3 mm), except for four events (05/23/17, 5/26/15, 6/24/15 and 7/9/15), which generated disproportionally large runoff volumes not clearly linked to the rainfall intensity. The resulting event volumetric runoff coefficients ranged from 0.00 to 2.68 (median $C_v = 0.03$). For the GI site, very long lag times were recorded (>9.13 hours) and can be attributed to flows lasting well after the cessation of rainfall, which were likely caused by interflow (lateral water movement through the unsaturated zone) and shallow groundwater seepage in the catchment. It is noteworthy that during the 2015 monitoring period, characterized by a relatively wet summer, soil water, likely originating from interflow, seeped into the collector swale from the side slope below the parking lot. That likely contributed to increased swale flows and total runoff volumes (see Figure 3(a)), and the presence of minor swale flows hours after the rainfall events ended.

Typically, the first rainfall intensity peaks were either entirely adsorbed by the catchment pervious areas or their runoff was significantly attenuated and delayed. As soil saturation progressed during continuous rainfall, these effects became less pronounced. The greatest runoff peak flow attenuation, during a storm event with a measurable outflow, was recorded during the 4.5-year storm event.

The rise of groundwater table during rainfall events greatly varied, ranging from 0 to 2.19 m. The maximum value of 2.19 m was recorded on 17 September 2015 during a 25-mm event lasting 40 hours. The soil water content also varied greatly at some sensor locations, with the range of recorded values varying from 2.3 to 56.6 Vol.-%. The initial soil water content (SWC_i) of individual events was much less variable and was calculated as 24.7 $\pm$ 2.6 Vol.-% (i.e., the median $\pm$ the absolute deviation). The change in the soil water content over the course of a storm event moderately varied: the median equalled 3.9 Vol.-%, with a minimum and maximum range from 0 to 11.2 Vol.-%.

The box plots of V, q_{max} and t_{lag} in Figure 4 represent the distribution of the data and extreme values for the CD site and the GI site (Figure 4(a)–4(c)). Except for q_{max}, the other two parameters V and t_{lag} exhibit a much larger spread at the GI site compared to the CD site, indicating a higher variability of the hydrological response. The data appears to be more (positively) skewed for V and t_{lag} compared to the CD data, but for q_{max} it shows a smaller spread and skewness, reflecting the mitigating effect of the GI site on peak flows. The locations of the median lines in the interquartile range box indicate significant differences among the three hydrological response parameters and between the two sites.

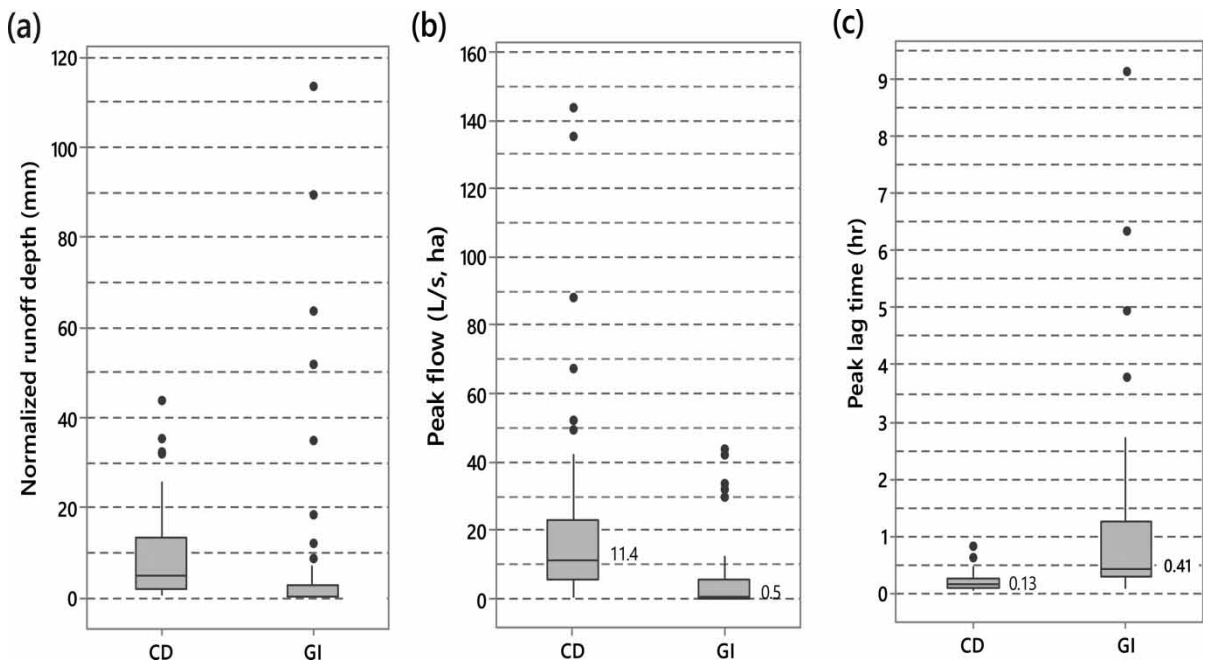

Figure 4 | (a)–(c) Box plots of the normalized runoff depth and peak flow, and peak lag time, serving to compare the CD- and GI sites. The median is shown beside the line within the interquartile range box.

Downloaded from http://iwaponline.com/wst/article-pdf/86/11/2777/1149397/wst086112777.pdf
by LULEA TEKNISKA UNIVERSITET user

Finally, all other measured and computed hydrological variables are summarized in Table 4. Complete details of event data are listed in Table SI in the supplementary material.

Hydrologic performance of the GI site

Runoff volume reduction

The shapes of the non-exceedance probability plots of event volumetric runoff coefficients show a clear distinction between the two sites, demonstrating the differences between the CD and GI drainage systems (Figure 5) and the roles of hydrologic abstractions and interflow in runoff formation, in the case of GI. Event volumes for the CD site appear to follow a lognormal distribution, while the GI points follow a sharp S-curve on the logarithmic scale.

At the CD site, a full conversion of rainfall into surface runoff was not exceeded for 90% of events, while at least 50% conversion of the rainfall volume into runoff ($C_v = 0.5$) occurred in 95% of all events. In the GI catchment, 41% of all events were completely captured without any runoff (represented by the points on the abscissa) and $C_v = 1.0$ was exceeded by about 10% of all events.

The median event volumetric runoff coefficients differed significantly between the CD site, $C_{v,med} = 0.87$, and the GI site with $C_{v,med} = 0.03$, as shown in Table 6. Total runoff volume reduction of the GI site was 96% when compared to the CD site, which follows from the number of fully captured storms and significant runoff attenuation in the remaining cases.

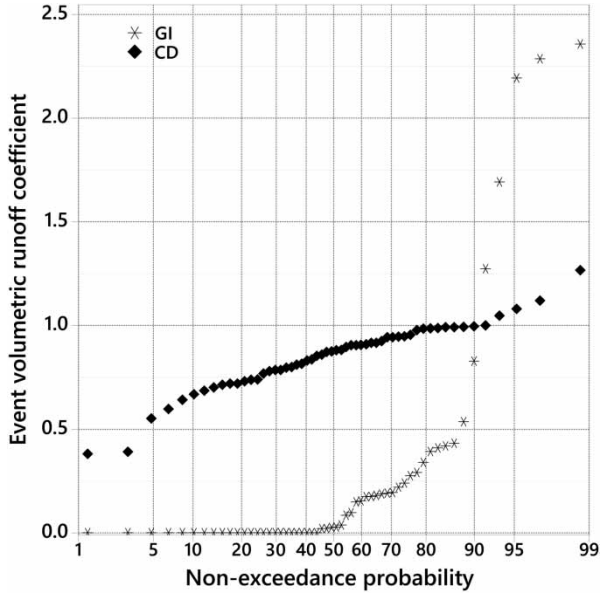

Figure 5 | Probability of non-exceedance of the event volumetric runoff coefficients for the CD system and the GI drainage.

Table 5 | Comparison of hydrologic response characteristics of the CD and GI sites

Statistical distribution parameter	C_v		Volume reduction e_v	Wilcoxon significance of difference[a]	Peak flow reduction e_q	Wilcoxon significance of difference q_{max}	Peak lag reduction e_{lag}	Wilcoxon significance of difference t_{lag}
	CD	GI		$N = 56$		$N = 56$		$N = 30$
Minimum	0.38	0.00	−1.77	W = 1,364 $p = 4.00 \times 10^{-7}$ Confidence 95.02%	−0.65	W = 1,442 $p = 1.53 \times 10^{-7}$ Confidence 95.02%	−0.43	W = 2, $p = 2.24 \times 10^{-06}$ Confidence 94.93%
25% quartile	0.73	0.00	0.70		0.94		0.51	
Median	**0.87**	**0.03**	**0.96**		**0.99**		**0.66**	
75% quartile	0.94	0.27	1.00		1.00		0.89	
Maximum	1.63	2.68	1.00		1.00		0.99	

Negative values denote flows in excess of rainfall input.
[a]Calculated by means of Minitab 18.

Downloaded from http://iwaponline.com/wst/article-pdf/86/11/2777/1149397/wst086112777.pdf
by LULEA TEKNISKA UNIVERSITET user

Table 6 | Spearman rho correlation matrix of associations among hydrologic factors and response parameters for the GI site

		P (mm)	*Dur* (h)	*i-5* (mm/h)	*i-avg* (mm/h)	*ADD* (days)	*IGL* (cm)	*MGL* (cm)	SWC_i (m^3/m^3)	*ΔSWC* (qm/qm)	*T* (degC)
Dur	R_s	**0.618**									
	p-value	0									
i-avg	R_s	**0.507**	−0.262								
	p-value	0	0.043								
i-5	R_s	**0.611**	0.213	0.527							
	p-value	0	0.102	0							
ADD	R_s	−0.014	−0.113	0.074	−0.065						
	p-value	0.913	0.388	0.575	0.622						
IGL	R_s	0.045	−0.116	0.091	0.035	0.31					
	p-value	0.733	0.376	0.487	0.792	0.016					
MGL	R_s	−0.42	−0.478	−0.052	−0.293	0.241	**0.714**				
	p-value	0.001	0	0.692	0.023	0.064	0				
SWC_i	R_s	0.022	0.298	−0.191	−0.202	−0.278	**−0.704**	**− 0.563**			
	p-value	0.869	0.024	0.155	0.132	0.036	0	0			
ΔSWC	R_s	**0.889**	**0.538**	0.38	**0.517**	− 0.047	−0.018	−0.47	0.113		
	p-value	0	0	0.004	0	0.731	0.894	0	0.402		
T	R_s	−0.016	−0.281	0.244	0.408	0.176	0.378	0.202	**−0.715**	− 0.045	
	p-value	0.907	0.034	0.068	0.002	0.19	0.004	0.132	0	0.738	
RH	R_s	0.095	0.201	−0.115	−0.092	−0.168	−0.303	−0.217	0.462	0.129	**−0.568**
	p-value	0.482	0.135	0.392	0.497	0.212	0.022	0.105	0	0.337	0

Moderate to high correlation Spearman rho values are bolded.

Runoff volumes in excess of rainfall volumes (i.e., negative reductions) occurred in the GI catchment more often than in the CD catchment, and were likely caused by interflow and drainage of the catchment subarea between the edge of the parking lot and the collector swale (Figure 2).

Concerning the factors influencing runoff volume reductions, moderate negative associations were found for the depth of rainfall (Spearman rho $R_s = 0.685$), with greater rainfall depths resulting in lower stormwater retention. Greater volume reductions occurred for smaller initial soil wetness (lower SWC_i; $R_s = -0.565$), indicating the capacity of dry soils to abstract and store more water. Volume reductions were also negatively correlated to intra-event increases of SWC (ΔSWC; $R_s = 0.606$), which indicates that the upper soil matrix is measurably contributing to runoff retention, as also reported earlier by Rujner *et al.* (2018). Other moderate associations affecting runoff volume reductions were found for *MGL* ($R_s = 0.574$), which confirms that shallow groundwater table reduces the hydrologic performance of the low-lying swale by inhibiting further infiltration, but not affecting the infiltration slope area located at a higher elevation.

Peak flow reduction

Probability distributions of peak flows for both types of drainage, CD and GI, show similar behaviour (Figure 6), but for equal probabilities, the CD site always produced higher peak flows. In agreement with the distribution of runoff coefficients, the probability of non-exceedance of zero flow was about 40% for the GI site.

The peak flows significantly differed between the two sites. Peak flows in GI were reduced by 99% (median), compared to those at the CD site and including the events with a complete capture of runoff (see Table 5). Considering only the events for which both sites generated outflow, the median peak flow reduction between the CD and GI sites was 94%. Data outliers occurred in the case of events with increased soil moisture saturation caused by the groundwater inflow.

Concerning the factors influencing peak flow reductions, moderately negative associations were found for the rainfall depths ($R_s = -0.659$), but not for rain durations or intensities. Thus, the peak flows increased only when the GI site was

Downloaded from http://iwaponline.com/wst/article-pdf/86/11/2777/1149397/wst086112777.pdf
by LULEA TEKNISKA UNIVERSITET user

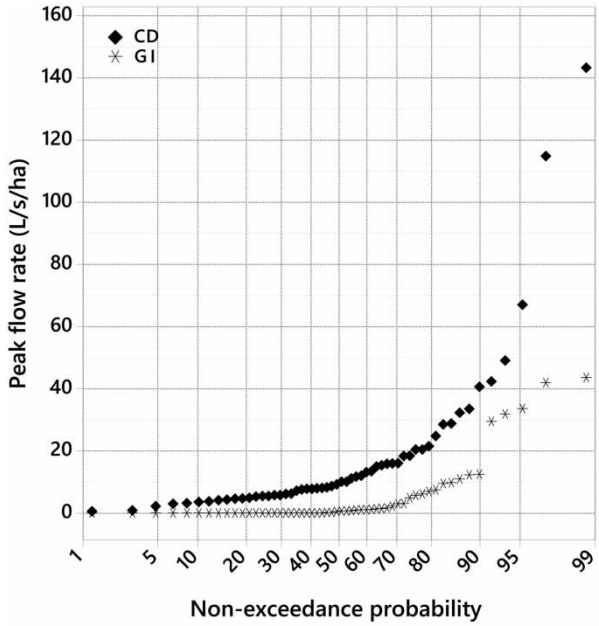

Figure 6 | Non-exceedance probability of peak flow rates for the parking lots for 56 events 2015–2019.

exposed to sufficient inputs of rainwater volumes, but not because of the duration of storm events, or the occurrence of short high-intensity rainfall bursts.

The negative correlation of ΔSWC ($R_s = -0.614$) with peak reductions indicates that as the soil infiltration capacity is declining, it is absorbing less water, and higher peak flows can be generated and vice versa. Other potential explanations would be high SWC_i or insufficient inflows. In a similar way as in the case of runoff volume reductions, the change in groundwater level during the event also affected the peak flows, as indicated by moderately high correlation to MGL ($R_s = 0.519$) (see Table S1 in supplementary material). In other words, the closer the groundwater table is to the surface, the greater runoff peaks may occur in the studied GI catchment.

Peak lag

The non-exceedance probability distributions of peak lag times differed greatly between the two sites (Figure 7). While lag times of the CD site were almost lognormally distributed, the distribution for GI seemed to follow almost a quasi-exponential trend. For the CD site, half of the events exhibited the peak lags shorter than 10.2 minutes, while for the same probability, the GI peak lags were three times longer than at the CD site. The median peak lag time for the GI site was significantly greater than for the CD site, with $t_{lag\ OD} = 24.6$ minutes compared to $t_{lag\ CD} = 7.8$ minutes, respectively. The lag times of the GI site were also more variable than the CD lag times. None of the tested factors was identified as exerting influence on the peak lag.

It was noted with interest that statistical analysis has not produced any evidence of the antecedent dry days' (ADD) influence on the catchment hydrologic response for the events sampled. For the tested 60 storm events, the median ADD of 1.6 days (maximum 11.4 days) appeared too short to allow a significant recovery of the water retention capacity.

Finally, air temperature and relative humidity also had no measurable effect on runoff formation at the GI site.

Associations among less influential factors

Spearman rho analysis indicated that environmental factors, which only showed insignificant, or no, correlations with the hydrologic performance of the GI site, can be influential for other factors and, thereby, exert indirect effects on the runoff response (see Table 6).

One example of association of less influential factors is SWC_i, which was negatively correlated with MGL. Thus, the higher groundwater levels (i.e., closer to the ground surface) are more likely to occur when the SWC_i was high. IGL and MGL are naturally associated with each other in such a way that lower initial groundwater levels will result in lower intra-event

Downloaded from http://iwaponline.com/wst/article-pdf/86/11/2777/1149397/wst086112777.pdf
by LULEA TEKNISKA UNIVERSITET user

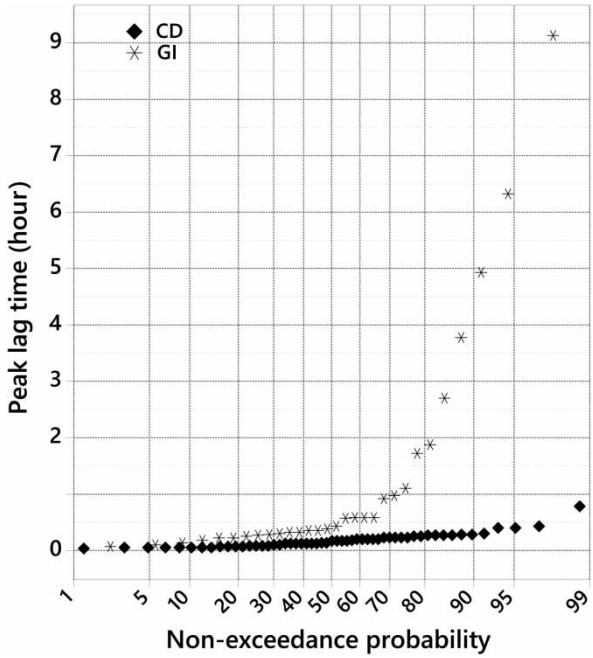

Figure 7 | Non-exceedance probability plots of peak lag times for both sites (CD and GI).

groundwater level maxima. A connection between high SWC_i and shallow groundwater would also support the observed occurrences of soil water seepage into the swale.

The SWC_i was correlated only to the runoff volume reductions at the GI site, but not to the peak flow reductions or the lag times. The SWC_i itself is influenced by temperature. The intra-event increase of SWC was independent of the SWC_i and appeared to be correlated only to rainfall (depth, duration, and average intensity). Scatter plots of hydrological factors versus the performance indicators are shown in Figure S1 (supplementary material).

DISCUSSION

Full-scale field monitoring and the paired-catchments experimental design used in this study provide essential information on the functioning of GI and the hydrologic benefits over conventional stormwater drainage, and in this context, cannot be fully replaced by modelling studies. Yet, the adopted approach presents a number of inherent challenges in the interpretation of results, as described below.

The first challenge stems from the fact that surface runoff from the catchment studied was greatly attenuated by a cascade of three infiltration features (the gravel strip, the sloping infiltration area, and the collector swale), which could not be monitored individually, but only as a single integrated unit. Hence, our study has not produced performance data for the individual features, but demonstrated that strong attenuation of surface runoff can be achieved by combining multiple features.

In the unimproved pervious part of the GI site, elevated hydrologic abstractions occurred even though the soils in this region were assessed by SGU (2018) as having generally low permeability. At the same time, it can be assumed that the fractured rock and debris layer, and preferential flows, played a major role in the initial runoff reduction. Furthermore, the pervious area of the GI catchment is large enough (50% of the catchment area) and ground irregularities contributing to depression storage too abundant to allow the conversion of rain peaks into runoff peaks during short rainfall bursts. Thus, it should be noted that the runoff volume reductions reported in our study resulted from a combined action of three infiltration features, the gravel strip, infiltration slope and swale, and frequently exceeded the runoff attenuation results from other studies usually dealing with grassed swales or filter strips. Consequently, our study results may not be directly comparable with typical GI field studies, addressing runoff volume reductions, for example, just by roadside grass swales, and reported in the literature in the range from 30% (Rushton 2001) to 47% (Barrett 2005). In another study of drainage performance of an unimproved GI, consisting of a road embankment and a ditch, Ahearn & Tveten (2009) also reported very high

Downloaded from http://iwaponline.com/wst/article-pdf/86/11/2777/1149397/wst086112777.pdf
by LULEA TEKNISKA UNIVERSITET user

runoff volume reductions, with 79% of the runoff volume infiltrated and the peak flows attenuated by 72–90%. Thus, the GI hydrological performance is expected to vary from site to site, reflecting numerous differences in site-specific characteristics, such as the type of facility, including its detailed geometry and infiltration features, hydraulic conductivity of facility soils, interactions with shallow groundwater, drainage patterns, and climatic factors.

Concerning the rainfall-runoff ratios of the 60 events studied, a median volumetric runoff coefficient of 0.03 was computed for the GI catchment (see Table 6) and fits within the range of volumetric runoff coefficients of urban soils (0.00–0.17) draining directly into the concrete storm drainage systems as reported by Pitt (1999). In the case of four storm events, the measured volume of event runoff exceeded the calculated input of rainwater to the catchment, as also reported in several earlier studies (Rushton 2001; Yu *et al.* 2001; Davis *et al.* 2012). Such seemingly anomalous results can be explained by entry of indeterminable varying subsurface interflow, originating outside of the surface runoff contributing area, into open drainage during peak flows causing otherwise 'unconnected' areas to contribute additional flows (Davis *et al.* 2012). Furthermore, undercatch of the study rain gauge would also contribute to higher values of the volumetric runoff coefficient.

Our observations of the GI drainage suggested periodical interactions of shallow groundwater with the catchment soil moisture, affecting the unsaturated zone and resulting in water exfiltration, even during dry days. The groundwater observations at the upstream end of the swale indicated that the potentiometric surface of the groundwater could rise up to 0.5 m above the swale bottom, at the lower end. Another source of exfiltration of soil water into the swale was the infiltration sloped area, which was initially (2015) only sparsely vegetated and without significant evapotranspiration, and the infiltrating runoff would contribute to enhanced interflows into the collector swale. Because of these dynamic changes of the catchment hydrology, runoff travel times were distributed randomly and likely contributed to some unexpected characteristics of the GI hydrologic performance. For example, the long peak lag times appeared to be caused by the delayed inflows into the collector swale, which were linked to soil saturation excess and/or groundwater exfiltration and, therefore, did not appear related to rainfall peaks over the catchment. The identified correlation between the maximum groundwater level (*MGL*) and elevated SWC_i and a potential effect on runoff formation can be hypothesized to be related to the level of soil saturation that causes gravitational water movement towards the saturated zone (exceedance of the soil matrix potential) occurring earlier during the rain event and attenuating the first runoff peak. Effects of shallow groundwater on GI performance were reported by Zhang & Chui (2019), who noted that runoff control by vegetated filter strips was affected by groundwater levels 0.0 to 2.0 m below the ground, because of the influence of groundwater on the initial soil moisture, and such influence was more significant in the case of lower-permeability soils, as in our case.

On the other hand, dry initial soil conditions facilitate water storage in the upper soil layers and thereby impede a groundwater table rise during the event. However, the lack of events with significant rainfall peak intensities in the sample set of monitored events could also partly explain the lack of statistical relationships between the peak flow reductions and storm durations or short, high-intensity rainfall bursts.

Temperature may indirectly affect the runoff formation at the study site, because it influences the SWC_i. The following indirect effects of temperature on runoff may be assumed: (i) Infiltration rates increase with higher temperature producing lower viscosity of water, (ii) higher temperatures cause higher vapour pressures in the air, resulting in higher rain intensity (1 °C → 7% increase in rain intensity; Hernebring *et al.* (2012)), explaining the predominantly low rain intensities in the study area, and (iii) lower ambient temperatures decrease evaporation of soil water (Philip & de Vries 1957), which may limit the role of evaporation in the hydrology of GI in cold climates. Consequently, *ADDs* (antecedent dry days), previously suggested to affect GI hydrologic performance by Winston *et al.* (2019), did not correlate, whereas SWC_i moderately correlated with the runoff volumes from the study site. The missing effect of *ADD* might also be explained by the climate of the region, in which the study site is located – relatively low temperatures and evapotranspiration rates even in summer, and frequent rain events.

As typical for field studies, the data analysis and interpretation were limited by the scope of rainfall events that were successfully monitored and represented a sample of the rainfall data at the study location. For comparing the two catchments, GI and CD, and the interpretation of data for runoff formation at the GI drainage site, only one event with a return period comparable to those of design storms (1–20-year return periods) has been recorded, but most of the events sampled were characterized by low to moderate rainfall intensities. However, frequently occurring events, with shorter return periods, bear significance for the water balance at the studied sites and for the design of stormwater management based on interception and on-site control of all events up to the 95th percentile event characterized by the 24-h rainfall depth (U.S. EPA 2009).

Downloaded from http://iwaponline.com/wst/article-pdf/86/11/2777/1149397/wst086112777.pdf
by LULEA TEKNISKA UNIVERSITET user

The implemented GI drainage at the study site yielded economic and environmental benefits. Among the former, one could name elimination of needs for a conventional storm sewer system, including installation of about 250 m of new concrete sewer pipes and a dozen of appurtenance structures in a difficult terrain. Environmental benefits include reduced export of pollutants with runoff from the parking lot to the receiving stream and reduced impacts of drainage discharges on erosion, morphology and physical habitat in the receiving stream environment. Finally, construction of the conventional sewer system would have caused a significant disturbance of the local environment in the study area.

CONCLUSIONS

A paired-catchment study of two commercial catchments, one with GI drainage and the other one with a conventional storm sewer system, served to compare and evaluate the hydrological performance of both systems, with primary focus on the GI catchment. The design of GI drainage focused on eliminating directly connected impervious areas by diverting runoff from asphalt surfaces onto a cascade of three pervious catchment elements, a gravel strip along the lower boundary of the parking lot, an infiltration slope area immediately below the strip, and a runoff collecting swale along the lower boundary of the catchment. Hydrological data comprising 60 storm events monitored in both catchments confirmed the benefits attained by implementing GI drainage: (i) significantly reduced runoff volumes and peak flows with median reductions of 96 and 99%, respectively, compared to conventional drainage; (ii) The reduced flows could be readily accommodated by the existing storm sewer system; (iii) Avoiding the cost of installing a conventional storm sewer system in the GI area, and the associated disturbance of the environment during construction. Open stormwater drainage also simplifies the maintenance of the drainage system, because potential obstructions occur on the catchment surface, where they can be easily noticed and removed without using special equipment. Finally, the study demonstrated that GI drainage can be successfully applied even in the challenging environment of the subarctic climate. On a cautionary note, in locations with shallow and varying groundwater levels the uncertainty of the GI runoff response can increase or limit the infiltration capacity and, therefore, potentially limit the attenuation of stormwater flows. The interdependence of environmental factors relevant for the formation of surface runoff in vegetated GI facilities further limits the predictability of drainage conveyance, compared to conventional drainage. Therefore, while these types of open GI systems can be robust and resilient substitutes for systems with DCIA, especially in low-density areas with affordable land, such as in peri-urban commercial or industrial areas, they would be less suitable for built-up urban centres.

ACKNOWLEDGEMENTS

The authors would like to gratefully acknowledge the help and support of the following partners: (i) The Municipality of Skellefteå, Department of Water and Wastewater, for providing the study sites and facilitating the setup of the monitoring station; (ii) Bo Hellgren and Mikael Carlsson, from the same department, for facilitating the municipal support; (iii) The LTU university colleagues, for assistance in instrumenting the study sites (Ralf Rentz), and maintaining and operating the sites (Ralf Rentz and Ico Broekhuizen); (iv) The project was conducted within the Stormwater & Sewers network supported by the Swedish Water and Wastewater Association (Svenskt Vatten).

FUNDING

The research was financed by Formas (Grant no. 2015-778) and VINNOVA (Swedish Governmental Agency for Innovation System) Drizzle – Centre for Stormwater Management (Grant no. 2016-05176).

AUTHOR CONTRIBUTION

Conceptualization, H.R.; Methodology, H.R., G.L., and K.F.; Validation, H.R., G.L., and J.M.; Formal Analysis, H.R.; Investigation, H.R.; Resources, M.V.; Data Curation, H.R..; Writing – Original Draft Preparation, H.R.; Writing – Review & Editing, G.L., K.F., and J.M.; Visualization, H.R.; Supervision, G.L, K.F., J.M., and M.V.; Project Administration, H.R..; Funding Acquisition, GL, J.M., and M.V.

DATA AVAILABILITY STATEMENT

All relevant data are included in the paper or its Supplementary Information.

Downloaded from http://iwaponline.com/wst/article-pdf/86/11/2777/1149397/wst086112777.pdf
by LULEA TEKNISKA UNIVERSITET user

CONFLICT OF INTEREST

The authors declare there is no conflict.

REFERENCES

Ahearn, D. & Tveten, R. 2009 Legacy LID: Stormwater treatment in unimproved embankments along highway shoulders in Western Washington. In: (She, N. & Char, M. (eds)), *Low Impact Development for Urban Ecosystem and Habitat Protection*, pp. 1–10. https://doi.org/10.1061/41009(333)19.

Alley, W. M. & Veenhuis, J. E. 1983 Effective impervious areas in urban runoff modelling. *Journal of Hydraulic Engineering* **109** (2), 313–319. https://doi.org/10.1061/(ASCE)0733-9429(1983)109:2(313).

Barrett, M. E. 2005 Performance comparison of structural stormwater best management practices. *Water Environment Research* **77** (1), 78–86. https://doi.org/10.2175/106143005X41654.

Beck, H. E., Zimmermann, N. E., McVicar, T. R., Vergopolan, N., Berg, A. & Wood, E. F. 2018 Present and future Köppen-Geiger climate classification maps at 1-km resolution. *Scientific Data* **5**, 180214.

City of Saskatoon 2012 *New Neighbourhood Design and Development Standards Manual. Section 6 – Storm Water Drainage System*. Available from: https://www.saskatoon.ca/business-development/development-regulation/specifications-standards/design-development-manual-new-neighbourhoods (accessed 13 June 2019).

Dahlström, B. 2010 *Regnintensitet – en molnfysikalisk betraktelse (Rain Intensity – A Cloud Physics Assessment)*. Report 2010–05 for the Swedish Water and Waste Water Association, Stockholm.

Davis, A. P., Stagge, J. H., Jamil, E. & Kim, H. 2012 Hydraulic performance of grass swales for managing highway runoff. *Water Research* **46** (20), 6775–6786. https://doi.org/10.1016/j.watres.2011.10.017.

Dingman, S. L. 2002 *Physical Hydrology*, 2nd edn. Waveland press, Prentice Hall, Long Grove, IL.

Geological Survey of Sweden (SGU). 2018 *Genomsläpplighet (Visningstjänst), Produktbeskriving, Dokumentversion 1.1. (Permeability (Viewing Service), Product Description, Document Version 1.1)* (accessed 13 June 2021).

Hernebring, C., Dahlström, B. & Kjellström, E. 2012 *Regnintensitet i Europa med fokus på Sverige – ett klimatförändringsperspektiv (Short Term Rainfall Intensities in Europe with the Focus on Sweden – A Climate Change Perspective)*. Report 2012–16 for the Swedish Water and Wastewater Association, Stockholm.

Hood, M. J., Clausen, J. C. & Warner, G. S. 2007 Comparison of stormwater lag times for low impact and traditional residential development 1. *JAWRA Journal of the American Water Resources Association* **43** (4), 1036–1046. https://doi.org/10.1111/j.1752-1688.2007.00085.x.

Jacobson, C. 2011 Identification and quantification of the hydrological impacts of imperviousness in urban catchments: a review. *Journal of Environmental Management* **92** (6), 1438–1448. https://doi.org/10.1016/j.jenvman.2011.01.018.

Minitab 18 2010 *Computer Software*. Minitab, Inc, State College, PA. Available from: www.minitab.com.

Muste, M., Lee, K. & Bertrand-Krajewski, J. L. 2012 Standardized uncertainty analysis for hydrometry: a review of relevant approaches and implementation examples. *Hydrological Sciences Journal* **57** (4), 643–667. https://doi.org/10.1080/02626667.2012.675064.

Obropta, C. C. & Del Monaco, N. 2018 Reducing directly connected impervious areas with green stormwater infrastructure. *Journal of Sustainable Water in the Built Environment* **4** (1), 05017004. https://doi.org/10.1061/JSWBAY.0000833.

Philip, J. R. & de Vries, D. A. 1957 Moisture movement in porous materials under temperature gradients. *Eos, Transactions American Geophysical Union* **38** (2), 22–232. https://doi.org/10.1029/TR038i002p00222.

Pitt, R. E. 1999 Small storm hydrology and why it is important for the design of stormwater control practices. *Journal of Water Management Modeling*. https://doi.org/10.14796/JWMM.R204-04.

Roy, A. H. & Shuster, W. D. 2008 Assessing impervious surface connectivity and applications for watershed management. *Journal of the American Water Resources Association* **45** (1), 198–209. https://doi.org/10.1111/j.1752-1688.2008.00271.x.

Rujner, H., Leonhardt, G., Marsalek, J., Perttu, A. M. & Viklander, M. 2018 The effects of initial soil moisture conditions on swale flow hydrographs. *Hydrological Processes* **32** (5), 644–654. https://doi.org/10.1002/hyp.11446.

Rushton, B. T. 2001 Low-impact parking lot design reduces runoff and pollutant loads. *Journal of Water Resources Planning and Management* **127** (3), 172–179. https://doi.org/10.1061/(ASCE)0733-9496(2001)127:3(172).

Schueler, T. R., Fraley-McNeal, L. & Cappiella, K. 2009 Is impervious cover still important? review of recent research. *Journal of Hydrologic Engineering* **14** (4), 309–315. https://doi.org/10.1061/(ASCE)1084-0699(2009)14:4(309).

Silva, M. C. & Silva, G. B. L. 2020 Cumulative effect of the disconnection of impervious areas within residential lots on runoff generation and temporal patterns in a small urban area. *Journal of Environmental Management* **253**, 109719. https://doi.org/10.1016/j.jenvman.2019.109719.

SMHI (Swedish Meteorological and Hydrological Institute) 2019 *Dataserier med Normalvärden för Perioden 1961–1990 (Data Series of Normal Values for the Period 1961–1990)*. Available from: https://www.smhi.se/data/meteorologi/dataserier-med-normalvarden-1.7354 (accessed online 28 May 2020).

Taguchi, V. J., Weiss, P. T., Gulliver, J. S., Klein, M. R., Hozalski, R. M., Baker, L. A. & Nieber, J. L. 2020 It is not easy being green: recognizing unintended consequences of green stormwater infrastructure. *Water* **12** (2), 522. https://doi.org/10.3390/w12020522.

Downloaded from http://iwaponline.com/wst/article-pdf/86/11/2777/1149397/wst086112777.pdf
by LULEA TEKNISKA UNIVERSITET user

U.S. EPA 2009 *Technical Guidance on Implementing the Stormwater Runoff Requirements for Federal Projects Under Section 438 of the Energy Independence and Security Act*. U.S. EPA, Office of Water, Washington, D.C, report EPA 841-B-09-001. Available from: https://www.epa.gov/sites/default/files/2015-08/documents/epa_swm_guidance.pdf (accessed 7 January 2022). https://doi.org/10.1111/j.1752-1688.2008.00271.x.

U.S. EPA 2020 *What is Green Infrastructure?* Available from: https://www.epa.gov/green-infrastructure/what-green-infrastructure (accessed 1 May 2021).

Walsh, C., Roy, A. H., Feminella, J. W., Cottingham, P. D., Groffman, P. M. & Morgan, R. P. 2005 The urban stream syndrome: current knowledge and the search for a cure. *Journal of the North American Benthological Society* **24** (3), 706–723. https://doi.org/10.1899/04-028.1.

Winston, R. J., Powell, J. T. & Hunt, W. F. 2019 Retrofitting a grass swale with rock check dams: hydrologic impacts. *Urban Water Journal* **16** (6), 404–411. https://doi.org/10.1080/1573062X.2018.1455881.

Ying, J., Zhang, X., Zhang, Y. & Bilan, S. 2021 Green infrastructure: systematic literature review. *Economic Research-Ekonomska Istraživanja*, 343–366. https://doi.org/10.1080/1331677X.2021.1893202.

Yu, S. L., Kuo, J. T., Fassman, E. A. & Pan, H. 2001 Field test of grassed-swale performance in removing runoff pollution. *Journal of Water Resources Planning and Management* **127** (3), 168–171. https://doi.org/10.1061/40430(1999)167.

Zhang, K. & Chui, T. F. M. 2019 A review on implementing infiltration-based green infrastructure in shallow groundwater environments: challenges, approaches, and progress. *Journal of Hydrology* **579**, 124089. https://doi.org/10.1016/j.jhydrol.2019.124089.

First received 26 June 2022; accepted in revised form 5 November 2022. Available online 21 November 2022

Downloaded from http://iwaponline.com/wst/article-pdf/86/11/2777/1149397/wst086112777.pdf
by LULEA TEKNISKA UNIVERSITET user